Applied Physiology, Nutrition, and Metabolism

Article

The effects of regional quadriceps architecture on angle-specific rapid force expression

Dustin J. Oranchuk[a,b,c], **William G. Hopkins**[b], **John B. Cronin**[a], **Adam G. Storey**[a], **and André R. Nelson**[b]

[a]Sports Performance Research Institute New Zealand, Health and Environmental Sciences, Auckland University of Technology, Auckland, New Zealand; [b]Institute for Health and Sport, Victoria University, Melbourne, Australia; [c]Muscle Morphology, Mechanics, and Performance Laboratory, Department of Physical Medicine and Rehabilitation, University of Colorado Anschutz Medical Campus, Aurora, CO, US

Corresponding author: **Dustin J. Oranchuk** (email: dustinoranchuk@gmail.com)

Abstract

Evaluating anatomical contributions to performance can increase understanding of muscle mechanics and guide physical preparation. While the impact of anatomy on muscular performance is well studied, the effects of regional quadriceps architecture on rapid torque or force expression are less clear. Regional (proximal, middle, and distal) quadriceps (vastus lateralis, rectus femoris, and vastus intermedius) thickness (MT), pennation angle (PA), and fascicle length (FL) of 24 males (48 limbs) were assessed via ultrasonography. Participants performed maximal isometric knee extensions at 40°, 70°, and 100° of knee flexion to evaluate rate of force development from 0 to 200 ms ($RFD_{0\text{-}200}$). Measurements were repeated on three occasions with the greatest $RFD_{0\text{-}200}$ and mean muscle architecture measures used for analysis. Linear regression models predicting angle-specific $RFD_{0\text{-}200}$ from regional anatomy provided adjusted correlations ($\sqrt{adjR^2}$) with bootstrapped compatibility limits. Mid-rectus femoris MT ($\sqrt{adjR^2} = 0.41$–0.51) and proximal vastus lateralis FL ($\sqrt{adjR^2} = 0.42$–0.48) were the best single predictors of $RFD_{0\text{-}200}$, and the only measures to reach precision with 99% compatibility limits. Small simple correlations were found across all regions and joint angles between $RFD_{0\text{-}200}$ and vastus lateralis MT ($\sqrt{adjR^2} = 0.28 \pm 0.13$; mean ± SD), vastus lateralis FL ($\sqrt{adjR^2} = 0.33 \pm 0.10$), rectus femoris MT ($\sqrt{adjR^2} = 0.38 \pm 0.10$), and lateral vastus intermedius MT ($\sqrt{adjR^2} = 0.24 \pm 0.10$). Between-correlation comparisons are reported within the article. Researchers should measure mid-region rectus femoris MT and vastus lateralis FL to efficiently and robustly evaluate potential anatomical contributions to rapid knee extension force changes, with distal and proximal measurements providing little additional value. However, correlations were generally small to moderate, suggesting that neurological factors may be critical in rapid force expression.

Key words: muscle architecture, length–tension, rectus femoris, torque, vastus intermedius, vastus lateralis

Introduction

Measures of muscle size (e.g., muscle thickness (MT), cross-sectional area, volume) and architecture (e.g., pennation angle (PA), fascicle length (FL)) have become commonplace when assessing acute or chronic effects of exercise (McMahon et al. 2014; Guex et al. 2016; Oranchuk et al. 2021*b*), baseline characteristics of performance, or clinical populations (Maden-Wilkinson et al. 2019; Handsfield et al. 2022; Tay and Kong 2022). Several research groups have also aimed to understand the effect of muscle architecture on function and performance (Green and Gabriel 2012; Wakahara et al. 2013; Ando et al. 2014; Trezise et al. 2016; Maden-Wilkinson et al. 2019; Chiu and Daehlin 2021; Maden-Wilkinson et al. 2021; Oranchuk et al. 2021*a*; Werkhausen et al. 2022), often with the intent of guiding exercise prescription relating to contraction type or other variables (Guilhem et al. 2013; Blazevich et al. 2014; McMahon et al. 2014; Kawama et al. 2021; Oranchuk et al. 2021*b*). For example, Oranchuk et al. (2021*b*) compared the acute effects of eccentric and eccentric quasi-isometric resistance exercise on quadriceps muscle architecture and reported differing regional MT and echo intensity changes, which may relate to long-term adaptations. Kawama et al. (2021) recently examined the relationship between regional muscle size of the hamstrings and isometric and concentric knee-flexion and hip-extension strength in healthy young men. Hip-extension force had the largest correlation with distal biceps femoris long head ($r = 0.53$–0.64) and semitendinosus ($r = 0.57$) cross-sectional area (Kawama et al. 2021). In contrast, biceps femoris short head ($r = 0.59$–0.68) and semimembranosus ($r = 0.57$–0.58) cross-sectional area were better predictors of knee-flexion strength (Kawama et al. 2021). These findings suggest that specific training strategies, such as force application using specific joint angles or contraction types, or fully utilizing the bi-articular arrangement of some muscles (Watanabe et al. 2021), may help produce specific architectural adaptations that could improve mechanical performance (Franchi et al. 2017, 2018*b*; Oranchuk et al. 2019).

While the relationships between muscle architecture and maximal force or torque expression are well studied (Green and Gabriel 2012; Wakahara et al. 2013; Ando et al. 2014; Trezise et al. 2016; Maden-Wilkinson et al. 2019, 2021; Chiu and Daehlin 2021; Oranchuk et al. 2021*a*; Werkhausen et al. 2022), very few studies have utilized rapid force or torque expression as a variable, possibly due to larger measurement variabilities (Oranchuk et al. 2022). Additionally, early-stage (0–100 ms) force and torque expression are poorly correlated with muscle size and architecture (Maden-Wilkinson et al. 2021; Werkhausen et al. 2022). For example, Maden-Wilkinson et al. (2021) examined the relationships between rapid torque production and anatomical variables such as quadriceps volume, PA, and FL, and patellar tendon moment arm. The authors found that despite muscle volume holding moderate-to-strong correlations with late-stage (≥100 ms) "explosive" torque, no substantial relationships were apparent at earlier epochs. Additionally, Coratella et al. (2020) examined the relationships between the rate of force development at several epochs and the muscle architecture of the vastus lateralis, vastus medialis, rectus femoris, and vastus intermedius. The correlations logically increased with larger epochs, with the greatest correlations between the rate of force development and vastus intermedius MT ($r = 0.27$–0.69), vastus lateralis FL ($r = 0.37$–0.63), and vastus intermedius FL ($r = 0.34$–0.64) (Coratella et al. 2020). While Coratella et al. (2020) were, to our knowledge, the first to examine the relationship between quadriceps architecture and rapid force expression, only the mid-region of each muscle and a single joint angle were examined. Also, several findings from Coratella et al. (2020) run contrary to our previous study (Oranchuk et al. 2021*a*) that demonstrated smaller correlations between mid-region vastus intermedius MT and maximal isometric torque ($\sqrt{\text{adj}R^2} = 0.23$–$0.42$).

Another gap in the literature is the examination of the relationships between anatomical variables and joint angle-specific mechanical outputs. With few exceptions (Oranchuk et al. 2021*a*), nearly all relevant correlational studies included a single joint angle (Blazevich et al. 2009; Green and Gabriel 2012; Ando et al. 2014; Trezise et al. 2016; Maden-Wilkinson et al. 2019; Trezise and Blazevich 2019; Coratella et al. 2020; Kawama et al. 2021). However, the length–tension relationship may have applications in performance, injury prevention, and rehabilitation (Escamilla et al. 2012; Lui et al. 2017; Yamauchi and Koyama 2019). Additionally, to our knowledge, the lone study, including isometric contractions at multiple joint angles, reports only peak torque (Oranchuk et al. 2021*a*). While Oranchuk et al. (2021*a*) reported little difference in correlations between joint angles, it remains to be determined if similar findings would exist when assessing the rate of torque development despite peak and rapid torque and force often being highly inter-related (Maffiuletti et al. 2016).

While several researchers have examined the relationships between anatomy and isometric force or force–time characteristics, none have determined the strength of association between regional architecture and rapid force expression at multiple joint angles. Therefore, we aimed to determine the relationships between regional quadriceps muscle architecture and rate of force development throughout the length–tension relationship. Based on previous research, we hypothesized that mid and distal vastus lateralis and lateral vastus intermedius MT and distal vastus lateralis FL would be the strongest predictors of rapid force expression. Additionally, we hypothesized that joint angle would not substantially affect the form-to-function relationship. The present study's findings could guide researchers and practitioners toward utilizing specific resistance-training techniques that may preferentially change regional muscle architecture (Zabaleta-Korta et al. 2020; Kassiano et al. 2022; Pedrosa et al. 2022) and improve neuromuscular performance for sports or rehabilitation.

Materials and methods

Experimental design

Using a repeated measures design, we examined measures of regional quadriceps anatomical parameters and rate of force development from 0 to 100 ms ($RFD_{0\text{-}100}$) and 0 to 200 ms ($RFD_{0\text{-}200}$) at a range of joint angles. Each participant was tested on three separate occasions, separated by 5–8 days. At each session, an ultrasonographic assessment of regional quadriceps MT, PA, and FL, followed by an isometric assessment of RFD at 40°, 70°, and 100° of knee flexion (0° = full extension), was completed. Inter-session reliability was determined for all measures. Average muscle architecture was used for analysis to minimize daily fluctuations in hydration and sonographer error. In contrast, the greatest RFD for each knee angle across all sessions was used for analysis to reduce variation associated with motivation and muscular activation differences between efforts that could not be quantified via electromyography.

Participants

Twenty-four healthy males (mean ± SD: 28.5 ± 4.7 years, 180.1 ± 7.7 cm, 81.6 ± 11.8 kg) volunteered for this study. All were categorized into tier 2 (trained/developmental) or 3 (highly trained/national level) as defined by McKay et al. (2022), as we wanted to examine participants with substantial muscle hypertrophy. As such, participants were required to have at least 6 months of resistance-training experience (6.73 ± 4.83, range: 1–18 years), with at least two weekly sessions of lower-body resistance training (2.54 ± 0.75, range: 2–5 sessions·week^{-1}), and be free of any musculoskeletal injuries for at least 3 months before data collection. Participants were instructed to maintain their current level of physical activity throughout the data collection period apart from refraining from strenuous physical activity, alcohol, caffeine, and other ergogenic aids for at least 48 h before each session. During each of the three sessions, ultrasonographic assessments of regional muscle architecture and multi-angle isometric torque measurements were collected for both dominant (determined by asking the participants which leg they would use to kick a ball) and non-dominant limbs. The Auckland University of Technology Research Ethics Committee approved the study (18/232) and all subjects provided written informed consent. All ethical considerations were in

line with the World Medical Association and the Declaration of Helsinki (Goodyear et al. 2007).

Testing procedures

Ultrasonography

All ultrasound images were collected using the same transducer and built-in software (45 mm linear array, GE Healthcare, Vivid S5, Chicago, IL). Ultrasound settings (frequency, 12 MHz; brightness, maximum; gain, 60 dB; dynamic range, 70; depth, individualized) were recorded and kept consistent across all sessions. All assessments were performed by the same sonographer with ~3 years of experience. Upon arrival, participants were positioned supine on a massage table for 15 min to allow fluid re-distribution (Varanoske et al. 2019). The participants remained supine with knees and hips fully extended (Aagaard 2003; Bradshaw et al. 2010; Noorkoiv et al. 2010; Maffiuletti et al. 2016; Koral et al. 2020; Tay and Kong 2022) with a foot strap used to prevent excessive external rotation. During this period, the participants had each thigh measured and marked by an International Society for the Advancement of Kinanthropometry (ISAK) level-2 anthropometrist. The length of the lateral aspect of the thigh was determined by measuring the distance from the superior border of the greater trochanter to the inferior border of the lateral condyle of the femur. The anterior aspect of the thigh was determined by measuring the distance between the superior border of the patella and the inferior border of the anterior, superior iliac spine (Noorkoiv et al. 2014). Thigh lengths were recorded and markings were made at 30% (proximal), 50% (middle), and 70% (distal) of the lateral and anterior distances, respectively (Oranchuk et al. 2020*c*). The vastus lateralis was marked by determining the most lateral aspect of the thigh.

Participants were instructed to briefly tense the quadriceps so that the researcher could mark the rectus femoris. Pilot testing with our resistance-trained male cohort determined that extended field-of-view scans of the vastus intermedius were not consistently clear. Thus, scanning depths were adjusted only to capture the vastus lateralis and rectus femoris muscles. The vastus medialis was excluded as it can be further broken down into the obliquus and longus portions, with deep and superficial fiber bundles (Castanov et al. 2019). Furthermore, MT of the vastus medialis oblique and longus has substantially smaller correlations with magnetic resonance imaging-derived cross-sectional area when compared to the vastus lateralis or rectus femoris (Giles et al. 2005). MT and PA of the vastus lateralis and lateral vastus intermedius, and the rectus femoris and anterior vastus intermedius were collected in the same snap-shot images, respectively. Typical proximal, middle, and distal lateral and anterior images are provided in Fig. 1.

The extended field-of-view function measured FL as extensively detailed previously (Noorkoiv et al. 2010; Oranchuk et al. 2020*a*). The ultrasound probe was moved across a muscle, while a texture mapping algorithm merged the sequence of images into a composite image (Noorkoiv et al. 2010; Franchi et al. 2018*a*). A water-soluble gel was applied to the scanning head of the ultrasound probe to achieve acoustic coupling, with care taken to avoid tissue deformation (Noorkoiv et al. 2010; Franchi et al. 2018*a*; Oranchuk et al. 2020*a*). The probe was perpendicular to the skin and parallel to the estimated fascicle direction (Noorkoiv et al. 2010; Franchi et al. 2018*a*; Oranchuk et al. 2020*a*). Two images were captured for each region or extended field-of-view scan. Two measurements for MT and two fascicles were assessed for both PA and FL from each image, and the mean was calculated (i.e., image mean). Each assessed fascicle must have been fully visible in each extended field-of-view scan. The mean of the two image means was then calculated and used for subsequent analyses (Oranchuk et al. 2020*a*).

Isometric dynamometry

Following the ultrasonographic assessment, participants warmed up by cycling at low-to-moderate resistance using a self-selected pace for 5 min (Oranchuk et al. 2022). Subjects were seated on the isokinetic dynamometer (CSMi; Lumex, Ronkonkoma, NY) at a hip angle of 85°, with shoulder, waist, and thigh straps to reduce body movement during contractions (Oranchuk et al. 2020*b*, 2022). The shin pad was positioned ~5 cm superior to the ankle joint malleoli (Oranchuk et al. 2022). Subjects were required to hold handles at the sides of the chair, while the non-working limb was set behind a restraining pad (Oranchuk et al. 2022). Knee alignment was determined by visual inspection and unloaded knee extensions. Dynamometer settings were recorded and matched for subsequent sessions.

Once fitted to the dynamometer, subjects underwent a series of extensions and flexions of the knee to determine safety stop positions and calibrate gravity correction (Oranchuk et al. 2022). Subjects then completed a standardized warm-up of concentric contractions of 30%, 50%, 70%, 85%, and 100% of perceived maximal voluntary contraction (Oranchuk et al. 2022). One minute after the completion of warm-up contractions, the participants' knee was positioned at 40° of flexion, where one familiarization isometric knee extension at 50% of perceived maximum torque was performed (Oranchuk et al. 2022). Sixty seconds later, two maximal contractions lasting 4 s were completed, with 30 s separating each contraction (Oranchuk et al. 2022). Participants were instructed to contract "as fast and hard as possible," following a countdown of "3-2-1-go!" (Maffiuletti et al. 2016; Oranchuk et al. 2022). All participants were given strong verbal encouragement and visual feedback of the torque–time tracing during each trial (Maffiuletti et al. 2016; Oranchuk et al. 2022). Participants were instructed to avoid any pre-tension and countermovement of the knee extensors, while the examiner carefully inspected the live torque–time trace leading up to each contraction (Maffiuletti et al. 2016; Oranchuk et al. 2022). The cut-off for pre-tension was set at 10 Nm (Oranchuk et al. 2022). Any contractions with a countermovement or an unsteady baseline were rejected and repeated (Maffiuletti et al. 2016; Oranchuk et al. 2022). The participants then completed the same series at 70° and 100° of knee flexion. The isometric contractions were always performed in series from 40° to 100° to avoid greater muscle damage and fatigue synony-

Fig. 1. Representative proximal, middle, and distal B-mode ultrasound images of the lateral (top) and anterior (bottom) quadriceps muscles. MT, muscle thickness; PA, pennation angle.

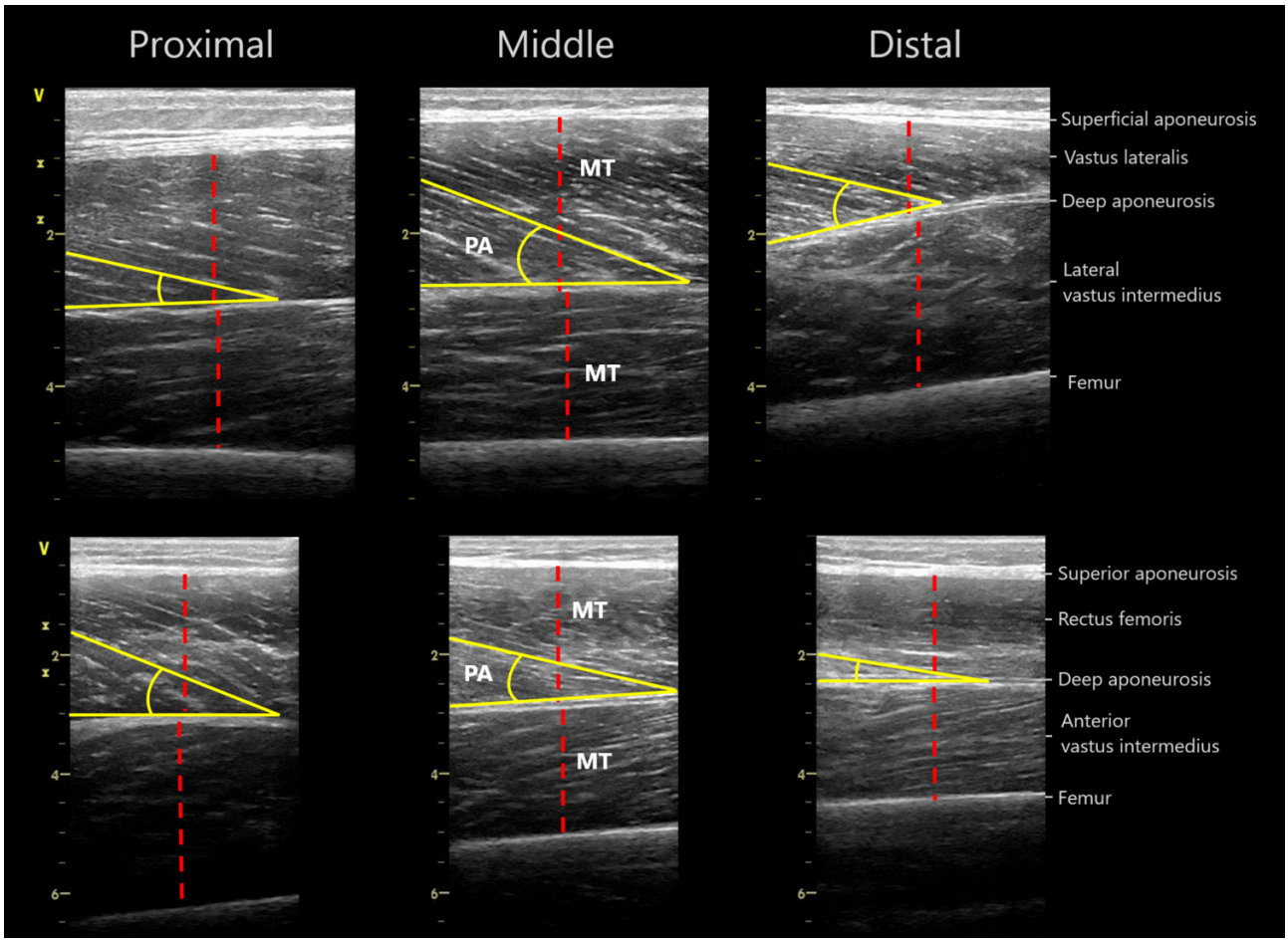

mous with long-muscle length contractions (Noorkoiv et al. 2014). Ten minutes following the final isometric contraction, the concentric warm-up and isometric assessments were repeated on the opposite limb. Limb order was randomized throughout the testing sessions and counterbalanced over the participant group. All contractions were collected, without filtering, via custom-made software (LabVIEW; National Instruments, New Zealand) sampling at 2000 Hz (Maffiuletti et al. 2016; Oranchuk et al. 2022).

Data processing and analysis

Ultrasonography

Images were stored and analyzed via digitizing software (ImageJ; National Institutes of Health). MT (cm) was defined as the perpendicular distance between the deep and superficial aponeurosis, and PA was defined as the angle of the fascicles relative to the deep aponeurosis (Franchi et al. 2018*a*). Due to the depth of the muscle, the fascicles on the lateral and anterior vastus intermedius were not consistently visible (Oranchuk et al. 2020*a*). Therefore, PA and FL were not recorded for the lateral and anterior vastus intermedius. As the rectus femoris is complex, in that there are distinctly different directions of pennation (Noorkoiv et al. 2014), only 23/48 of the distal rectus femoris FL measurements could be determined. Representative vastus lateralis and rectus femoris-extended field-of-view images are illustrated in Figs. 2A and 2B, respectively. Anatomical variables were averaged across all sessions to reduce errors arising from sonography or participant variability.

Isometric dynamometry

Data were analyzed via a customized MATLAB (MathWorks, Natick, MA) script. As the moment arm substantially affects isometric outputs (Green and Gabriel 2012; Varanoske et al. 2019), all torque data (Newton meters) were divided by the length of the dynamometer arm, in meters, to obtain force (Newtons) based on the formula below:

$$\text{Force} = \frac{\text{Torque}}{\text{Moment Arm}}$$

This procedure normalizes the difference in shank length between participants, providing a better proxy of muscular capacity in isolation (Varanoske et al. 2019). As such, all knee extension kinetics are reported in Newtons per sec-

Fig. 2. Representative extended field-of-view images of the vastus lateralis with proximal, middle, and distal fascicle lengths (A). Typical extended field-of-view image of the rectus femoris (B); note the lack of discernible fascicles toward the distal region. FL, fascicle length.

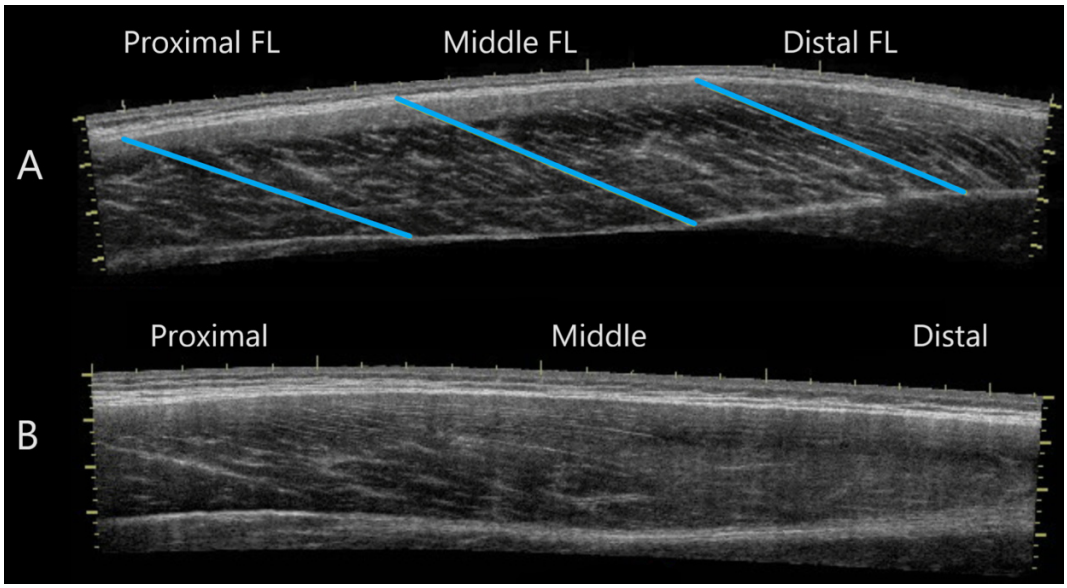

ond ($N \cdot s^{-1}$). After adjusting for dynamometer lever length, force outputs over 200 N were identified to signify a full contraction and eliminate false contractions with efforts falling under this threshold considered submaximal. The onset of force was determined through visual inspection and a manual section of each force–time curve (Maffiuletti et al. 2016; Oranchuk et al. 2022). The same researcher determined onset of force by visually detecting the last trough before force deflected above the range of the baseline noise (Maffiuletti et al. 2016; Oranchuk et al. 2020*a*). The rates of force development were quantified as the linear slope of the force/time relationship. The contraction with the highest RFD was analyzed. The maximum values of $RFD_{0\text{-}100}$ and $RFD_{0\text{-}200}$ across the three sessions were utilized to reduce errors arising from submaximal voluntary activation.

Statistical analysis

Reliability

Measures of RFD, MT, and FL were log-transformed before analysis to reduce non-uniformity of error (Hopkins 2000; Hopkins et al. 2009) and analyzed with an Excel spreadsheet (Hopkins 2015). Following log transformation, data were visually confirmed to be normally distributed. Only measures with sufficiently high intersession reliability were included in the correlational analysis to minimize bias in the correlations between variables. Since the mean or maximum of the three sessions was used in the correlation analysis, the intraclass correlation coefficient (ICC [type 3,1]) of the mean of the three sessions was used as the measure of interest (Hopkins et al. 2009). A value of ICC $>$ 0.75 was considered sufficiently reliable (Bradshaw et al. 2010). Compared with other studies, the between-session typical error of measurement (TEM) was also analyzed and expressed as a percentage for RFD, MT, and FL (Hopkins 2000; Hopkins et al. 2009). TEM is expressed in degrees for PA, as there is an upper limit of 90°, and unlike other measures, the error would not be expected to increase with increasing values (Hopkins 2000; Hopkins et al. 2009).

While not a primary aim of the study, the variability of intra-image measures (e.g., the variability of two proximal vastus lateralis FL measures in the same image) was performed to determine variations in quadriceps anatomy across regions and muscles using the same procedure and interpretation as for the intrasession reliability analysis. Intra-image variability statistics was not analyzed for RFD as the greatest value, regardless of contraction or session, was utilized for the correlational analysis.

Correlational analysis

As the primary goal was to examine the effects of regional quadriceps anatomy on RFD, a measure was included only if it was sufficiently reliable (ICC $>$ 0.75) in all three regions (proximal, middle, and distal) and knee joint angles (40°, 70°, and 100°). Simple linear regressions were used to predict angle-specific RFD with anatomical parameters in isolation (e.g., distal vastus lateralis MT). Multiple linear regressions were used to determine if the difference in predictive ability between regions (e.g., distal vastus lateralis FL vs. middle vastus lateralis FL) was substantial. Thus, the multiple regression analysis (detailed below) provides the associations between the single correlations of a single muscle to give readers the best single region(s) to assess in clinical or research practices.

All regression analyses were performed with "PROC REG statement" in the Statistical Analysis Software (University Edition of SAS Studio, version 9.4, SAS Institute, Cary NC). Measures of the ability of the regression models to predict RFD were the multiple R (the correlation between observed and predicted values), $\sqrt{R^2}$ (equivalent to the absolute value

of Pearson's *r* for a single predictor), and the adjusted multiple *R* (the square-root of the *R*-squared, $\sqrt{\text{adj}R^2}$, adjusted for degrees of freedom). The adjustment removes the upward bias in the *R*-squared that occurs when any predictor is added to a model with finite sample size (Ezekiel 1930). Negative values of $\text{adj}R^2$ were expressed as negative correlations by changing the sign before taking the square root. Effects (adjusted multiple *R*, their means, and their differences) are presented with the qualitative magnitude of their observed (sample) value and interpreted as trivial, small, moderate, large, very large, and extremely large for values <0.10, ≥0.10, ≥0.30, ≥0.50, ≥0.70, and ≥ 0.90, respectively (Hopkins et al. 2009).

Reporting sampling uncertainty for effect estimates is recommended in various disciplines (Wilkinson 1999; Althouse et al. 2021), including sport and exercise science (Hopkins et al. 2009; Hopkins 2022). Sampling uncertainty in the effects estimates are presented as 90% compatibility limits (90%CL), which were estimated from percentiles of the effects in 10 000 bootstrapped samples. Bootstrapping was essential when the effect was the difference between two correlation coefficients, because the correlations come from the same subjects, and there is no simple formula for the standard error that would define the sampling distribution for such a statistic (Zhu 1997). The bootstrapped effects were estimated initially by performing multiple linear regression with each bootstrapped sample, but the median values of the effects were substantially higher than those in the original sample. Therefore, values in the bootstrapped samples were derived as follows: the regression coefficients in the original sample were used to predict the dependent variable in each bootstrapped sample; the correlation between the predicted and observed values of the dependent variable in each sample was squared and adjusted for degrees of freedom; the square root of this adjusted *R*-squared then provided values of adjusted multiple *R*, which showed close agreement between the original and bootstrapped median values. As a further check on the adequacy of this bootstrap method, the analyses were performed on simulated data with a sample size of 24 and simple correlations between a dependent variable and two predictor variables in two limbs. One hundred analyses of 10 000 bootstrap samples were performed for correlations ranging from 0.00 to 0.70. Observed and median-adjusted multiple *R* showed a downward bias of 0.05 to 0.10 for true correlations of 0.00–0.30, 0.04 for true correlations of 0.50, and only 0.02 for true correlations of 0.70. Despite the bias, 90%CLs showed less than the 10% expected error rate in their coverage of low values of true correlations and a slightly higher error rate (~12%) for true correlations of 0.50 and 0.70. We, therefore, judged bootstrapping to be trustworthy.

The non-clinical version of magnitude-based decisions with a minimally informative prior was used to interpret the uncertainty in effect magnitudes (Hopkins 2022). Chances that the true magnitude was a substantial negative value, a trivial value, and a substantially positive value were derived directly from the bootstrapped samples as the proportion of sample values with those magnitudes. Effects were deemed to have adequate precision if the chances of one or other substantial true values were <5% (i.e., the 90%CLs did not include substantial positive and negative values). Effects with adequate precision are reported with a qualitative descriptor for the magnitude with chances >25% using the following scale: >25%, possibly (*); >75%, likely (**); >95%, very likely (***); and >99.5%, most likely (****) (Hopkins et al. 2009). When the chances of a substantial magnitude were >95%, the magnitude itself is described as clear; this outcome is equivalent to rejection of the hypothesis that the effect was non-substantial (superiority or inferiority testing; (Hopkins 2022)), with *p*-value < 0.05 for very likely substantial and <0.005 for most likely substantial. Effects with inadequate precision are described as unclear. Effects with adequate precision defined by 99%CL are highlighted in **bold** in tables and figures; the overall error rate for coverage of 10 independent true values with such intervals is that of a single effect with a 90%CL (10%), and interpretation of outcomes is focused on these effects.

Results

Reliability

Intersession, intrasession, and intra-image (two fascicles from the same image) reliability of quadriceps architectural parameters have been previously reported in detail (Oranchuk et al. 2021*a*). In brief, all MT and vastus lateralis PA and FL measures were sufficiently reliable (ICC = 0.77–0.98). However, rectus femoris PA and FL were either unreliable or unable to be consistently evaluated in each participant and, therefore, not included in the correlational analysis.

$RFD_{0\text{-}100}$ was reliable across all limbs at 40° (ICC = 0.85, TEM = 15%), 70° (ICC = 0.79, TEM = 20%), and 100° (ICC = 0.80, TEM = 19%). $RFD_{0\text{-}200}$ was slightly more reliable at 40° (ICC = 0.90, TEM = 13%), 70° (ICC = 0.81, TEM = 15%), and 100° (ICC = 0.87, TEM = 12%). Furthermore, muscle architecture and RFD correlations were always trivially different between 0–100 and 0–200 epochs. Therefore, due to the very large number of correlations, and current evidence suggesting little-to-no relationship between early-stage rate of force development and muscle architecture (Maden-Wilkinson et al. 2021; Werkhausen et al. 2022), all subsequent in-text results are reported for $RFD_{0\text{-}200}$ only.

Correlational analysis

Mean regional anatomical measures are summarized in Table 1. $RFD_{0\text{-}200}$ for the dominant and non-dominant limbs were (mean ± SD) 2510 ± 657 $N{\cdot}s^{-1}$ and 2462 ± 599 $N{\cdot}s^{-1}$ at 40°, 2876 ± 873 $N{\cdot}s^{-1}$ and 2789 ± 725 $N{\cdot}s^{-1}$ at 70°, and 2388 ± 656 $N{\cdot}s^{-1}$ and 2319 ± 701 $N{\cdot}s^{-1}$ at 100°, respectively. All between-limb differences in predictive ability were unclear or possibly small; therefore, all correlations are presented after pooling dominant and non-dominant limbs.

Simple linear regressions

Correlations and bootstrapped 90%CLs of individual measures of regional muscle anatomy with $RFD_{0\text{-}200}$ at 40°, 70°, and 100° of knee flexion are presented in Fig. 3. Additionally, all simple correlations between $RFD_{0\text{-}100}$ and muscle architecture with 90%CLs are provided in Supplementary Table S1, while correlations for $RFD_{0\text{-}200}$ are provided in

Table 1. Regional quadriceps architecture averaged over three sessions.

Muscle	Measurement	Limb	Proximal	Middle	Distal
Vastus lateralis	MT (cm)	Dominant	2.54 ± 0.36	2.81 ± 0.43	2.21 ± 0.34
		Non-dominant	2.44 ± 0.33	2.74 ± 0.41	2.20 ± 0.37
	PA (°)	Dominant	17.1 ± 3.2	20.6 ± 2.6	22.7 ± 2.7
		Non-dominant	16.3 ± 2.7	20.2 ± 2.1	22.5 ± 2.8
	FL (cm)	Dominant	7.73 ± 0.68	8.18 ± 0.83	7.16 ± 0.83
		Non-dominant	7.70 ± 0.73	8.16 ± 0.72	7.12 ± 0.90
Rectus femoris	MT (cm)	Dominant	2.80 ± 0.26	2.69 ± 0.33	1.96 ± 0.30
		Non-dominant	2.76 ± 0.33	2.69 ± 0.31	1.99 ± 0.31
Lateral vastus intermedius	MT (cm)	Dominant	2.02 ± 0.44	2.04 ± 0.54	1.93 ± 0.44
		Non-dominant	2.01 ± 0.51	2.03 ± 0.53	1.84 ± 0.42
Anterior vastus intermedius	MT (cm)	Dominant	2.94 ± 0.46	2.24 ± 0.47	1.88 ± 0.42
		Non-dominant	2.96 ± 0.47	2.36 ± 0.49	1.78 ± 0.37

Note: MT, muscle thickness; PA, pennation angle; FL, fascicle length. Data are mean ± SD. Data are across 48 limbs.

Supplementary Table S2. Regardless of region or joint angle, small correlations were found between $RFD_{0\text{-}200}$ and vastus lateralis MT (mean ± SD $\sqrt{adjR^2} = 0.28 \pm 0.13$), vastus lateralis FL ($\sqrt{adjR^2} = 0.33 \pm 0.10$), rectus femoris MT ($\sqrt{adjR^2} = 0.38 \pm 0.10$), and lateral vastus intermedius MT ($\sqrt{adjR^2} = 0.24 \pm 0.10$). Neither vastus lateralis PA ($\sqrt{adjR^2} = 0.00 \pm 0.18$) nor anterior vastus intermedius ($\sqrt{adjR^2} = 0.06 \pm 0.12$) were substantially associated with $RFD_{0\text{-}200}$. The largest single correlation was between mid-rectus femoris MT and $RFD_{0\text{-}200}$ at 100° ($\sqrt{adjR^2} = 0.51$, 90%CL: 0.22–0.72), with mid-rectus femoris MT also having the greatest mean correlation with $RFD_{0\text{-}200}$ regardless of joint angle ($\sqrt{adjR^2} = 0.47 \pm 0.05$). This finding was followed by proximal vastus lateralis FL ($\sqrt{adjR^2} = 0.44 \pm 0.02$) and distal rectus femoris MT ($\sqrt{adjR^2} = 0.42 \pm 0.02$) as the only measures consistently correlating with $RFD_{0\text{-}200}$ ($\sqrt{adjR^2} \geq 0.40$). Additionally, middle rectus femoris MT and middle vastus lateral FL were the only measures to reach acceptable precision with 99%CIs at all three joint angles.

Regardless of model, correlations were greatest for $RFD_{0\text{-}200}$ at 100° ($\sqrt{adjR^2} = 0.24 \pm 0.15$) and decreased at 70° ($\sqrt{adjR^2} = 0.21 \pm 0.20$) and 40° ($\sqrt{adjR^2} = 0.15 \pm 19$). However, the differences were either unclear or possibly to likely trivial-small.

Between-correlation comparisons

Between-region differences in simple correlations are presented in Supplementary Table S3. Of the 54 between-region comparisons, 51 were trivial or small, with 36 decisions being unclear. Distal vastus lateralis MT had likely higher correlations with $RFD_{0\text{-}200}$ than proximal vastus lateralis MT at all joint angles ($\Delta\sqrt{adjR^2} = 0.22$–$0.27$). Likewise, mid vastus lateralis MT was likely better correlated to $RFD_{0\text{-}200}$ than proximal vastus lateralis MT at the 70° joint angle ($\Delta\sqrt{adjR^2} = 0.21$). Distal vastus lateralis PA had likely higher correlations with $RFD_{0\text{-}200}$ than proximal vastus lateralis PA at all joint angles ($\Delta\sqrt{adjR^2} = 0.33$–$0.39$). Distal vastus lateralis PA also had a possibly greater correlation to $RFD_{0\text{-}200}$ than mid vastus lateralis PA at the 100° joint angle ($\Delta\sqrt{adjR^2} = 0.27$). Middle vastus lateralis FL was likely and possibly better correlated to $RFD_{0\text{-}200}$ than distal vastus lateralis FL at 70° ($\Delta\sqrt{adjR^2} = 0.17$) and 100° ($\Delta\sqrt{adjR^2} = 0.27$), respectively. Middle vastus lateralis FL was also possibly better correlated with RFD than proximal vastus lateralis FL at 100° ($\Delta\sqrt{adjR^2} = 0.17$). Middle rectus femoris MT has possibly and likely higher correlations with $RFD_{0\text{-}200}$ than proximal rectus femoris MT at 40° ($\Delta\sqrt{adjR^2} = 0.14$) and 100° ($\Delta\sqrt{adjR^2} = 0.27$), respectively. Distal lateral vastus intermedius MT had likely higher correlations with $RFD_{0\text{-}200}$ proximal lateral vastus lateralis MT at 70° ($\Delta\sqrt{adjR^2} = 0.23$) and 100° ($\Delta\sqrt{adjR^2} = 0.26$), respectively. Distal lateral vastus lateralis MT was also possibly better correlated to $RFD_{0\text{-}200}$ than mid lateral vastus lateralis MT at 70° ($\Delta\sqrt{adjR^2} = 0.19$).

Discussion

While several studies have examined the effects of quadriceps anatomy on force or torque expression, none have investigated the relationship between regional architecture and rapid force expression at multiple joint angles. Our primary findings were that mid-region vastus lateralis FL and mid-region rectus femoris MT were the strongest and most consistent predictors of $RFD_{0\text{-}200}$. However, the correlations in the present study were generally small to moderate, with only rectus femoris MT and $RFD_{0\text{-}200}$ at 100° holding a large ($r = 0.51$) correlation, highlighting the relative importance of neural variables on rapid force production. When paired with previous findings (Oranchuk et al. 2021*a*), researchers should assess distal or mid vastus lateralis MT, mid rectus femoris MT, and mid vastus lateralis FL to estimate the knee extensors' potential for both maximal and rapid force expression.

A key finding of this study was the relatively high and consistent correlations between rectus femoris MT and $RFD_{0\text{-}200}$ ($\sqrt{adjR^2} = 0.25$–0.51). This finding contrasts with previous work demonstrating that rectus femoris MT ($\sqrt{adjR^2} = -0.01$–0.49) was a minor and inconsistent contributor to peak force when compared to vastus lateralis MT ($\sqrt{adjR^2} = 0.18$–0.64) or FL ($\sqrt{adjR^2} = 0.29$–0.60) (Oranchuk et al. 2021*a*). Several factors can most likely explain this discrepancy. While all

Fig. 3. Adjusted simple correlations with bootstrapped 90% compatibility limits of rate of force development (RFD) from 0 to 200 ms at 40°, 70°, and 100° of knee flexion with regional quadriceps architecture.

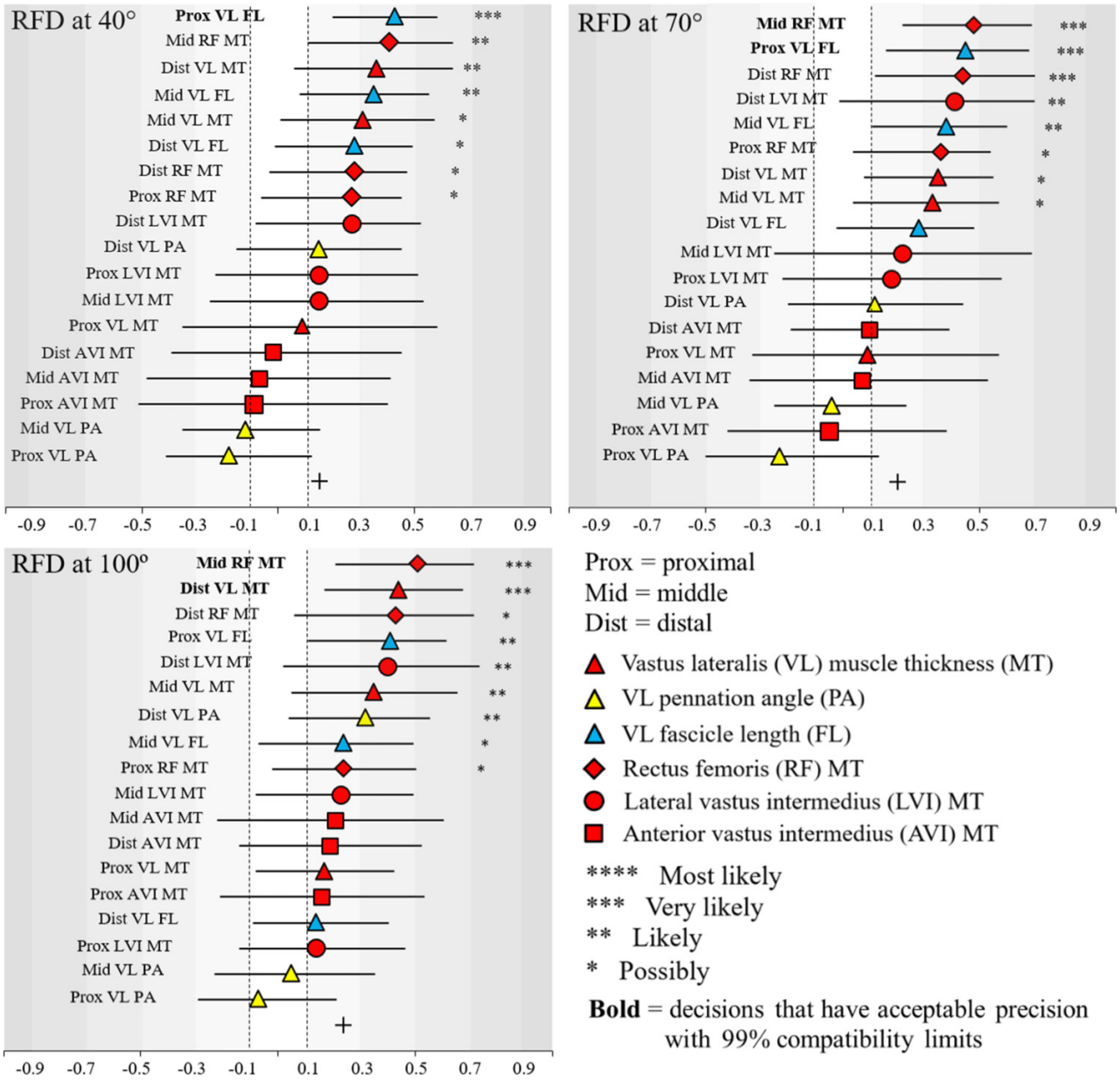

quadriceps muscles insert into the patella, the rectus femoris is oriented and attaches directly superior (Chiu and Daehlin 2021). Therefore, the rectus femoris has the most direct line of pull of the superior quadriceps muscles (Chiu and Daehlin 2021), potentially reducing the time required for measurable force following contraction onset. However, the rectus femoris is substantially smaller than the vastus lateralis, limiting its contribution to maximal knee extensor strength (Noorkoiv et al. 2014; Maden-Wilkinson et al. 2019; Kordi et al. 2020; Stock et al. 2020).

Vastus lateralis FL being a top, though modest, predictor of rapid force expression is logical given sarcomeres-in-series implication to contraction velocity (Boakes et al. 2007) or, more recently, sarcomere resting length theories (Pincheira et al. 2022). Though our hypothesis of distal vastus lateralis FL being a top predictor of RFD was not confirmed, mid-region FL had higher correlations at all three joint angles. It is difficult to determine why this is the case, especially as distal vastus lateralis FL was consistently the worst predictor of RFD of the FL measures. However, it is plausible that regional FL is representative of other regions of the same muscle. The mid-region of the vastus lateralis is also thicker than the proximal or distal regions and, therefore, likely has the greatest potential for maximal force expression (Oranchuk et al. 2020*a*). Given that maximal strength is a good predictor of rapid force expression (Cormie et al. 2011), our finding is logical. This finding is also interesting as distal vastus lateralis FL had the greatest inter-participant variability.

While distal vastus lateralis PA was moderately related to $RFD_{0\text{-}200}$ at 100° ($\sqrt{adjR^2} = 0.32$), all other correlations were trivial or small, with a relatively large range ($\sqrt{adjR^2} = -0.25$–0.13). This finding, similar to our previous work examining peak force (Oranchuk et al. 2021*a*), contradicts several studies examining maximal or rapid contractile performance (Wakahara et al. 2013; Trezise et al. 2016; Trezise and Blazevich 2019; Kordi et al. 2020). However, our findings are similar to a recent study also examining knee extension kinetics that found small correlations between vastus lateralis PA and rate of force development over several epochs ($r = -0.23$–0.19) (Coratella et al. 2020). Though it is difficult to determine the reasons for these conflicting results, it has recently been suggested that assessing PA may lack functional significance due to a variety of factors, including its relationship to MT and FL, changes in PA based on joint position and muscle force, and concepts such as muscle gearing (Lieber 2022). Whether PA may hold greater correlations with force if assessed in the same joint position has yet to be answered.

Contrary to Coratella et al. (2020), this study did not find large or consistent correlations between the RFD measure and vastus intermedius MT. The discrepancy between studies could be due to several factors. First, Coratella et al. (2020) utilized a relatively small sample of 17, whereas we examined 48 limbs across 24 individuals. Second, and similarly to Ando et al. (2014), Coratella et al. (2020) was only concerned with knee extensor capabilities and muscle architecture on a single occasion, inviting additional uncertainty. Additionally, while our participants were well-trained (≥2 lower body resistance-training sessions per week for ≥6 months), the participants in the aforementioned studies were "recreationally trained" and "healthy," respectively. Therefore, training status may have affected the correlational results as the force expression of the well-trained participants is likely more influenced by neural versus anatomical factors (Aagaard 2003). These differences in neural control would partially explain the generally weaker correlations in this present study compared to those of Coratella et al. (2020). However, this could be due to other factors, including Coratella and colleagues' use of a strain gauge. In contrast, an isokinetic dynamometer was used in this study. While Ando et al. (2014) reported greater correlations with force expression with the anterior aspect of the vastus intermedius, contrary to our present and previous findings (Oranchuk et al. 2021*a*), it is unclear if the anterior or lateral vastus intermedius was assessed by Coratella et al. (2020). Therefore, no consensus exists regarding which aspect of the vastus intermedius should be scanned. Finally, while we, and other researchers, have utilized several strategies to maximize reliability and determined good inter-rater variability, it cannot be assumed that sonographers are without substantive error.

Other researchers have determined that cross-sectional areas and muscle volume are stronger predictors of muscle function than MT (Franchi et al. 2018*a*). Therefore, it could be recommended that the distal and middle quadriceps cross-sectional area be assessed via panoramic ultrasound, magnetic resonance imaging, or computerized tomography to obtain a robust predictor of force expression in only two scans. A third scan examining mid-region vastus lateralis FL could also be performed if predicting RFD potential is a priority.

Limitations and future research directions

While the aims of this study were achieved, there are several limitations to consider. First, we employed a novel statistical approach to evaluate the associations between regional quadriceps muscle architecture and angle-specific $RFD_{0\text{-}200}$, challenging direct comparisons with previous literature. Second, the use of surface or needle electromyography to determine individual muscle activation at different joint angles was not utilized; yet similar examinations have reported electromyography to have trivial-to-moderate correlations to isometric (Trezise et al. 2016; Trezise and Blazevich 2019) and cycling performance (Kordi et al. 2020), and/or contributed little-to-multiple regression models (Green and Gabriel 2012; Trezise et al. 2016; Trezise and Blazevich 2019). Similarly, we could only evaluate our participants' voluntary efforts, not the maximal potential of the quadriceps musculature through peripheral or transcranial stimulation techniques (Lanza et al. 2017; Koral et al. 2020). While the aforementioned strategy to maximize voluntary activation removes many limitations, the lack of joint angle order randomization may have led to the accumulation of non-trivial fatigue levels as contractions progressed from 40° to 100° of flexion. We used the greatest RFD outputs over the three collection sessions to address this partially. It should be noted that we utilized a manual method to detect the onset of each contraction. However, there is ongoing debate regarding the relative advantages and limitations of manual detection versus mathematical algorithms (Maffiuletti et al. 2016). Finally, we converted torque to force by adjusting the raw outputs to the length of the lever arm. While this step was required to remove the effect of shank length (Green and Gabriel 2012; Varanoske et al. 2019), several relevant studies did not include this step (Blazevich et al. 2009; Wakahara et al. 2013; Noorkoiv et al. 2014; Trezise et al. 2016; Trezise and Blazevich 2019; Kawama et al. 2021; Werkhausen et al. 2022), making direct comparison difficult.

Future research could include the knee joint moment arm, which can change through the range of motion (Blazevich et al. 2009; Trezise et al. 2016; Maden-Wilkinson et al. 2021). However, like electromyography variables, the joint moment arm minimally contributes to multi-regression models (Trezise et al. 2016; Maden-Wilkinson et al. 2021). Compression of the dynamometer padding means that the joint angles reported were likely systematically overestimated and RFD was delayed. While prohibitively time-consuming in the present study, researchers may also wish to scan the quadriceps in the same position as the isometric strength assessment (Maden-Wilkinson et al. 2021; Werkhausen et al. 2022) to represent joint angle-specific architecture and muscle gearing better and improve correlations. More experienced sonographers or different hardware could have consistently produced extended field-of-view rectus femoris and vastus intermedius FLs, allowing for further elucidation of the relationship between regional quadriceps anatomy and angle-specific force. Likewise, sonographer error is an ever-

present consideration, and this study is no exception. Analyzing the mean FL over multiple regions may also result in interesting findings while diminishing the effect of sonographer error.

While several researchers have examined inhomogeneous morphological and architectural adaptations, very few have evaluated more than two regions of an individual muscle (Zabaleta-Korta et al. 2020). Therefore, we recommended that future investigations examine three or more regions to illuminate further the effect of training or disuse on region-specific muscle adaptations. Based on the results of the present study, it seems unlikely that changes in regional muscle architecture would directly result in altered rapid force expression. However, this theory requires investigation. The bi-articular structure and function of the rectus femoris should be further explored as it is the most commonly injured quadriceps muscle during accelerations and sprinting (McAleer et al. 2022), and may play a critical functional performance role in clinical populations (Watanabe et al. 2021). Other advanced methods, such as muscle volume assessments and region-specific high-density electromyography, may unveil additional insights.

Conclusions

This study was the first to examine the effect of regional quadriceps architecture on RFD at multiple joint angles. We found that the relative contribution of regional anatomical parameters to RFD does not change at different joint angles. However, middle and distal rectus femoris MT and mid-region vastus lateralis FL was the best, though modest, predictors of RFD, likely due to these respective muscles and structures having the most direct line of pull on the musculo-tendonous unit, and the greatest number of serial sarcomeres, respectively. Combined with previous research, ultrasonic evaluations of the quadriceps should focus on mid-region MT and FL of the vastus lateralis and mid-region rectus femoris MT to obtain a thorough yet time-efficient model of quadriceps force expression. However, the correlations were relatively small, suggesting that alterations in regional muscle architecture through the use of specific resistance-training strategies are unlikely to directly contribute to changes in rapid force expression.

Article information

History dates

Received: 21 February 2023
Accepted: 20 June 2023
Accepted manuscript online: 30 June 2023
Version of record online: 4 September 2023

Copyright

Data availability

Data generated or analyzed during this study are available from the corresponding author upon reasonable request.

Author information

Author contributions

Conceptualization: DJO
Data curation: DJO, WGH
Formal analysis: DJO, ARN
Funding acquisition: JBC
Investigation: DJO, ARN
Methodology: DJO, WGH
Project administration: DJO, JBC, AGS, ARN
Resources: JBC
Software: WGH
Supervision: JBC, AGS, ARN
Validation: DJO
Visualization: DJO
Writing – original draft: DJO
Writing – review & editing: DJO, JBC, AGS, ARN

Funding information

Dustin J. Oranchuk was supported by the Auckland University of Technology's Vice-Chancellors Doctoral Scholarship.

Supplementary material

Supplementary data are available with the article at https://doi.org/10.1139/apnm-2023-0074.

References

Aagaard, P. 2003. Training-induced changes in neural function. Exerc. Sport Sci. Rev. **31**(2): 61–67. doi:10.1097/00003677-200304000-00002. PMID: 12715968.

Althouse, A.D., Below, J.E., Claggett, B.L., Cox, N.J., de Lemos, J.A., Deo, R.C., et al. 2021. Recommendations for statistical reporting in cardiovascular medicine: a special report from the American Heart Association. Circulation, **144**(4): e70–e91. doi:10.1161/CIRCULATIONAHA.121.055393. PMID: 34032474.

Ando, R., Saito, A., Umemura, Y., and Akima, H. 2014. Local architecture of the vastus intermedius is a better predictor of knee extension force than that of the other quadriceps femoris muscle heads. Clin. Physiol. Funct. Imaging. **35**(5): 376–382. doi:10.1111/cpf.12173. PMID: 24915999.

Blazevich, A.J., Coleman, D.R., Horne, S., and Cannavan, D. 2009. Anatomical predictors of maximum isometric and concentric knee extensor moment. Eur. J. Appl. Physiol. **105**(6): 869–878. doi:10.1007/s00421-008-0972-7. PMID: 19153760.

Blazevich, A.J., Cannavan, D., Waugh, C.M., Miller, S.C., Thorlund, J.B., Aagaard, P., and Kay,, A.D. 2014. Range of motion, neuromechanical, and architectural adaptations to plantar flexor stretch training in humans. J. Appl. Physiol. **117**(5): 452–462. doi:10.1152/japplphysiol.00204.2014.

Boakes, J.L., Foran, J., Ward, S.R., and Lieber, R.L. 2007. Muscle adaptation by serial sarcomere addition 1 year after femoral lengthening. Clin. Orthop. Relat. Res. **456**: 250–253. doi:10.1097/01.blo.0000246563.58091.af. PMID: 17065842.

Bradshaw, E., Hume, P., Calton, M., and Aisbett, B. 2010. Reliability and variability of day-to-day vault training measures in artistic gymnastics. Sports Biomech. **9**(2): 79–97. doi:10.1080/14763141.2010.488298. PMID: 20806844.

Castanov, V., Hassan, S.A., Shakeri, S., Vienneau, M., Zabjek, K., Richardson, D., et al. 2019. Muscle architecture of vastus medialis obliquus and longus and its functional implications: a three-dimensional investigation. Clin. Anat. **32**(4): 515–523. doi:10.1002/ca.23344. PMID: 30701597.

Chiu, L.Z.F., and Daehlin, T.E. 2021. Three-dimensional modelling of human quadriceps femoris forces. J. Biomech. **120**(110347). PMID: 33711598.

Coratella, G., Longo, S., Borrelli, M., Christian, D., Ce, E., and Esposito, F. 2020. Vastus intermedius muscle architecture predicts the late phase of the knee extension rate of force development in recreationally resistance-trained men. J. Sci. Med. Sport. **23**(11): 1100–1104. doi:10.1016/j.jsams.2020.04.006. PMID: 32416973.

Cormie, P., McGuigan, M.R., and Newton, R.U. 2011. Developing maximal neuromuscular power: part 1—biological basis of maximal power production. Sports Med. **41**(1): 17–38. doi:10.2165/11537690-000000000-00000. PMID: 21142282.

Escamilla, R.F., Macleod, T.D., Wilk, K.E., Paulos, L., and Andrews, J.R. 2012. Anterior cruciate ligament strain and tensile forces for weight-bearing and non-weight-bearing exercises: a guide to exercise selection. J. Orthop. Sports Phys. Ther. **42**(3): 208–220. doi:10.2519/jospt.2012.3768. PMID: 22387600.

Ezekiel, M. 1930. Methods of correlational analysis. John Wiley, New York.

Franchi, M.V., Reeves, N.D., and Narici, M.V. 2017. Skeletal muscle remodeling in response to eccentric vs. concentric loading: morphological, molecular, and metabolic adaptations. Front. Physiol. **8**(447): 1–16. PMID: 28154536.

Franchi, M.V., Raiteri, B.J., Longo, S., Sinha, S., Narici, M.V., and Csapo, R. 2018a. Muscle architecture assessment: strengths, shortcomings and new frontiers of in vivo techniques. Ultrasound Med. Biol. **44**(12): 2492–2504. doi:10.1016/j.ultrasmedbio.2018.07.010. PMID: 30185385.

Franchi, M.V., Ruoss, S., Valdivieso, P., Mitchell, K.W., Smith, K., Atherton, P.J., et al. 2018b. Regional regulation of focal adhesion kinase after concentric and eccentric loading is related to remodelling of human skeletal muscle. Acta. Physiol. **223**(3): e13056. doi:10.1111/apha.13056.

Giles, L.S., Webster, K.E., McClelland, J.A., and Cook, J. 2005. Can ultrasound measurements of muscle thickness be used to measure the size of individual quadriceps muscles in people with patellofemoral pain? Phys. Ther. Sport **16**(1): 45–52. doi:10.1016/j.ptsp.2014.04.002.

Goodyear, M.D.E., Krleza-Jeric, K., and Lemmens, T. 2007. The declaration of Helsinki. Br. Med. J. **335**(7621): 624–625. doi:10.1136/bmj.39339.610000.BE.

Green, L.A., and Gabriel, D.A. 2012. Anthropometrics and electromyography as predictors for maximal voluntary isometric arm strength. J. Sport Health Sci. **1**(2): 107–113. doi:10.1016/j.jshs.2012.05.004.

Guex, K., Degache, F., Morisod, C., Sailly, M., and Millet, G.P. 2016. Hamstring architectural and functional adaptations following long vs. short muscle length eccentric training. Front. Physiol. **7**(340): 1–9. PMID: 26858649.

Guilhem, G., Cornu, C., Maffiuletti, N.A., and Guevel, A. 2013. Neuromuscular adaptations to isoload versus isokinetic eccentric resistance training. Med. Sci. Sports Exerc. **45**(2): 326–335. doi:10.1249/MSS.0b013e31826e7066. PMID: 22903139.

Handsfield, G.G., Williams, S., Khuu, S., Lichtwark, G.A., and Stott, N.S. 2022. Muscle architecture, growth, and biological remodelling in cerebral palsy: a narrative review. BMC. Musculoskelet. Disord. **23**(233): 1–17. PMID: 34980067.

Hopkins, W.G. 2000. Measures of reliability in sports medicine and science. Sports Med. **30**(1): 1–15. doi:10.2165/00007256-200030010-00001. PMID: 10907753.

Hopkins, W.G. 2015. Spreadsheets for analysis of validity and reliability. Sportscience. **19**: 36–44.

Hopkins, W.G. 2022. Replacing statistical significance and nonsignificance with better approaches to sampling uncertainty. Front. Physiol. **13**: 962132. doi:10.3389/fphys.2022.962132. PMID: 36267575.

Hopkins, W.G., Marshall, S.W., Batterham, A.M., and Hanin, J. 2009. Progressive statistics for studies in sports medicine and exercise science. Med. Sci. Sports Exerc. **41**(1): 3–12. doi:10.1249/MSS.0b013e31818cb278. PMID: 19092709.

Kassiano, W.L., De, Costa, D., De Londrina, U.E., Kunevaliki, G., De Londrina, U.E., and De Londrina, U.E. 2022. Greater gastrocnemius muscle hypertrophy after partial range of motion training carried out at long muscle lengths. J. Strength Cond. Res. Ahead of print.

Kawama, R., Okudaira, M., Maemura, H., and Tanigawa, S. 2021. Muscle- and region-specific associations between muscle size and muscular strength during hip extension and knee flexion in the hamstrings. J. Sport Rehabil. **30**(8): 1172–1177. doi:10.1123/jsr.2021-0007. PMID: 34426558.

Koral, J., Oranchuk, D.J., Wrightson, J.G., Twomey, R., and Millet, G.Y. 2020. Mechanisms of neuromuscular fatigue and recovery in unilateral versus bilateral maximal voluntary contractions. J. Appl. Physiol. **128**(4): 785–794. doi:10.1152/japplphysiol.00651.2019.

Kordi, M., Folland, J., Goodall, S., Haralabidis, N., Maden-Wilkinson, T., Sarika, P.T., et al. 2020. Mechanical and morphological determinants of peak power output in elite cyclists. Scand. J. Med. Sci. Sports, **30**(2): 227–237. doi:10.1111/sms.13570. PMID: 31598998.

Lanza, M.B., Balshaw, T.G., and Folland, J.P. 2017. Do changes in neuromuscular activation contribute to the knee extensor angle–torque relationship? Exp. Physiol. **102**(8): 962–973. doi:10.1113/EP086343. PMID: 28594464.

Lieber, R.L. 2022. Can we just forget about pennation angle. J. Biomech. **132**(6): 110954. doi:10.1016/j.jbiomech.2022.110954. PMID: 35074689.

Lui, Y., Sun, Y., Zhu, W., and Yu, J. 2017. The late swing and early stance of sprinting are most hazardous for hamstring injuries. J. Sport Health Sci. **6**(2): 133–136. PMID: 30356597.

Maden-Wilkinson, T.M., Balshaw, T.G., Massey, G., and Folland, J.P. 2019. What makes long-term resistance-trained individuals so strong? A comparison of skeletal muscle morphology, architecture, and joint mechanics. J. Appl. Physiol. **128**(4): 1000–1011. doi:10.1152/japplphysiol.00224.2019.

Maden-Wilkinson, T.M., Balshaw, T.G., Massey, G.J., and Folland, J. 2021. Muscle architecture and morphology as determinants of explosive strength. Eur. J. Appl. Physiol. **121**(4): 1099–1110. doi:10.1007/s00421-020-04585-1. PMID: 33458800.

Maffiuletti, N.A., Aagaard, P., Blazevich, A.J., Folland, J., Tillin, N., and Duchateau, J. 2016. Rate of force development: physiological and methodological considerations. Eur. J. Appl. Physiol. **116**(6): 1091–1116. doi:10.1007/s00421-016-3346-6. PMID: 26941023.

McAleer, S., Macdonald, B., Lee, J., Zhu, W., Giakoumis, M., Maric, T., et al. 2022. Time to return to full training and recurrence of rectus femoris injuries in elite track and field athletes 2010–2019; a 9-year study using the British Athletics Muscle Injury Classification. Scand. J. Med. Sci. Sports. **32**(7): 1109–1118. doi:10.1111/sms.14160. PMID: 35332596.

McKay, A.K.A., Stellingwerff, T., Smith, E.S., Martin, D.T., Mujika, I., Goosey-Tolfrey, V.L., et al. 2022. Defining training and performance caliber: a participant classification frameword. Int. J. Sports Physiol. Perform. **17**(2): 317–331. doi:10.1123/ijspp.2021-0451. PMID: 34965513.

McMahon, G.E., Morse, C.I., Burden, A., Winwood, K., and Onambele, G.L. 2014. Impact of range of motion during ecologically valid resistance training protocols on muscle size, subcutaneous fat, and strength. J. Strength Cond. Res. **28**(1): 245–255. doi:10.1519/JSC.0b013e318297143a. PMID: 23629583.

Noorkoiv, M., Stavnsbo, P., Aagaard, P., and Blazevich, A. 2010. In vivo assessment of muscle fascicle length by extended field-of-view ultrasonography. J. Appl. Physiol. **109**(6): 1974–1979. doi:10.1152/japplphysiol.00657.2010.

Noorkoiv, M., Nosaka, K., and Blazevich, A.J. 2014. Neuromuscular adaptations associated with knee joint angle-specific force change. Med. Sci. Sports Exerc. **46**(8): 1525–1537. doi:10.1249/MSS.0000000000000269. PMID: 24504427.

Oranchuk, D.J., Storey, A.G., Nelson, A.R., and Cronin, J.B. 2019. Isometric training and long-term adaptations; effects of muscle length, intensity, and intent: a systematic review. Scand. J. Med. Sci. Sports. **29**(4): 484–503.

Oranchuk, D.J., Nelson, A.R., Storey, A.G., and Cronin, J.B. 2020a. Variability of regional quadriceps architecture in trained men assessed by B-mode and extended-field-of-view ultrasonography. Int. J. Sports Physiol. Perform. **15**(3): 430–436. doi:10.1123/ijspp.2019-0050.

Oranchuk, D.J., Neville, J.G., Storey, A.G., Nelson, A.R., and Cronin, J.B. 2020b. Variability of concentric angle-specific isokinetic torque and impulse assessments of the knee extensors. Physiol. Meas. **41**(1): 01NT02. doi:10.1088/1361-6579/ab635e. PMID: 31851953.

Oranchuk, D.J., Stock, M.S., Nelson, A.R., Storey, A.G., and Cronin, J.B. 2020c. Variability of regional quadriceps echo intensity in active young men with and without subcutaneous fat correction. Appl.

Physiol. Nutr. Metab. **45**(7): 745–752. doi:10.1139/apnm-2019-0601. PMID: 31917597.

Oranchuk, D.J., Hopkins, W.G., Nelson, A.R., Storey, A.G., and Cronin, J.B. 2021a. The effect of regional quadriceps anatomical parameters on angle-specific isometric torque expression. Appl. Physiol. Nutr. Metab. **46**(4): 368–378. doi:10.1139/apnm-2020-0565. PMID: 33058713.

Oranchuk, D.J., Nelson, A.R., Storey, A.G., Diewald, S.N., and Cronin, J.B. 2021b. Short-term neuromuscular, morphological, and architectural responses to eccentric quasi-isometric muscle actions. Eur. J. Appl. Physiol. **121**(1): 141–158. doi:10.1007/s00421-020-04512-4. PMID: 32995961.

Oranchuk, D.J., Storey, A.G., Nelson, A.R., Neville, J.G., and Cronin, J.B. 2022. Variability of multiangle isometric force–time characteristics in trained men. J. Strength Cond. Res. **36**(1): 284–288. doi:10.1519/JSC.0000000000003405. PMID: 31593034.

Pedrosa, G.F., Lima, F.V., Schoenfeld, B.J., Lacerda, L.T., Simões, M.G., Pereira, M.R., et al. 2022. Partial range of motion training elicits favorable improvements in muscular adaptations when carried out at long muscle lengths. Eur. J. Sport Sci. **22**(8): 1250–1260. doi:10.1080/17461391.2021.1927199. PMID: 33977835.

Pincheira, P.P., Boswell, M.A., Franchi, M.V., Delp, S.L., and Lichtwark, G.A. 2022. Biceps femoris long head sarcomere and fascicle length adaptations after 3 weeks of eccentric exercise training. J. Sport Health Sci. **11**(1): 43–49. doi:10.1016/j.jshs.2021.09.002. PMID: 34509714.

Stock, M.S., Oranchuk, D.J., Burton, A.M., and Phan, D.C. 2020. Age-, sex-, and region-specific differences in skeletal muscle size and quality. Appl. Physiol. Nutr. Metab. **45**(11): 1253–1260. doi:10.1139/apnm-2020-0114. PMID: 32450045.

Tay, M.R.J., and Kong, K.H. 2022. Ultrasound measurement of rectus femoris and locomotor outcomes in patients with spinal cord injury. Life. **12**(7): 1073. doi:10.3390/life12071073. PMID: 35888161.

Trezise, J., and Blazevich, A.J. 2019. Anatomical and neuromuscular determinants of strength change in previously untrained men following heavy strength training. Front. Physiol. **10**: 1001. PMID: 31447693.

Trezise, J., Collier, N., and Blazevich, A.J. 2016. Anatomical and neuromuscular variables strongly predict maximum knee extension torque in healthy men. Eur. J. Appl. Physiol. **116**(6): 1159–1177. doi:10.1007/s00421-016-3352-8. PMID: 27076217.

Varanoske, A.N., Coker, N.A., Johnson, B.D.I., Belity, T., Mangine, G.T., Stout, J.R., et al. 2019. Effects of rest position on morphology of the vastus lateralis and its relationship with lower-body strength and power. Funct. Morphol. Kinesiol. **4**(3): 64. doi:10.3390/jfmk4030064.

Wakahara, T., Kanehisa, H., Kawakami, Y., Fukunaga, T., and Tanai, T. 2013. Relationship between muscle architecture and joint performance during concentric contractions in humans. J. Appl. Biomech. **29**(4): 405–412. doi:10.1123/jab.29.4.405. PMID: 22927507.

Watanabe, K., Vieira, T.M., Gallina, A., Kouzaki, M., and Moritani, T. 2021. Novel insights into bi-articular muscle actions gained from high-density EMG. Exerc. Sport Sci. Rev. **49**(3): 179–187. doi:10.1249/JES.0000000000000254. PMID: 33927163.

Werkhausen, A., Gløersen, O., Nordez, A., Paulsen, G., Bojsen-Møller, J., and Seynnes, O. 2022. Rate of force development relationships to muscle architecture and contractile behavior in the human vastus lateralis. Sci. Rep. **12**(1): 21816. doi:10.1038/s41598-022-26379-5. PMID: 36528647.

Wilkinson, L. 1999. Statistical methods in psychology journals: guidelines and explanations. Am. Psychol. **54**(8): 594–604. doi:10.1037/0003-066X.54.8.594.

Yamauchi, J., and Koyama, K. 2019. Relation between the ankle joint angle and the maximum isometric force of the toe flexor muscles. J. Biomech. **85**: 1–5. doi:10.1016/j.jbiomech.2018.12.010. PMID: 30712779.

Zabaleta-Korta, A., Fernández-Peña, E., and Santos-Concejero, J. 2020. Regional hypertrophy, the inhomogeneous muscle growth: a systematic review. Strength. Cond. J. **42**(5): 94–101. doi:10.1519/SSC.0000000000000574.

Zhu, W. 1997. Making bootstrap statistical inferences: a tutorial. Res. Q. Exerc. Sport. **68**(1): 44–55. doi:10.1080/02701367.1997.10608865. PMID: 9094762.